

# Mo K-Edge EXAFS and S K-Edge Absorption Studies of the Amorphous Molybdenum Sulfides MoS<sub>4.7</sub>, MoS<sub>3</sub>, and MoS<sub>3</sub>·nH<sub>2</sub>O (n ~ 2)

Simon J. Hibble,\* David A. Rice, David M. Pickup, and Michael P. Beer

Department of Chemistry, University of Reading, Whiteknights, P.O. Box 224, Reading RG6 6AD, U.K.

Received January 20, 1995<sup>®</sup>

Molybdenum K-edge EXAFS measurements on the new amorphous sulfide, MoS<sub>4.7</sub>, and the known amorphous sulfides, MoS<sub>3</sub> and MoS<sub>3</sub>·nH<sub>2</sub>O (n ~ 2), have yielded information on the coordination around molybdenum in these compounds. The results for MoS<sub>3</sub> and its hydrates, MoS<sub>3</sub>·nH<sub>2</sub>O (n = 1.7, 2.1, and 2.2), prepared using a number of different methods, show that the coordination around molybdenum is the same in all of these materials. In MoS<sub>3</sub> and MoS<sub>3</sub>·nH<sub>2</sub>O, molybdenum is surrounded by six sulfurs at ~2.43 Å and is also bonded to a molybdenum at 2.76 Å. No evidence was found for the longer Mo–Mo distance of ~3.2 Å in MoS<sub>3</sub> which has been reported by other workers. There is evidence that the Mo–S bond lengths are inequivalent but not as markedly different as has been suggested previously. Our results suggest that the models for MoS<sub>3</sub> presented in the literature to date may be incorrect. The local structure around molybdenum in MoS<sub>4.7</sub> differs from that in MoS<sub>3</sub>. The most important differences are that the average number of sulfur atoms around each molybdenum in MoS<sub>4.7</sub> is higher than in MoS<sub>3</sub> and that the Mo–Mo coordination number is greater. Our structural model for MoS<sub>4.7</sub> takes account of this with an average 7<sup>1</sup>/<sub>3</sub> sulfurs around each molybdenum and an average Mo–Mo coordination number of 1<sup>1</sup>/<sub>3</sub>. EXAFS analysis and infrared spectroscopy are consistent with the formulation of MoS<sub>3</sub> as Mo<sup>V</sup>(S<sup>2-</sup>)<sub>2</sub>(S<sub>2</sub><sup>2-</sup>)<sub>0.5</sub> and MoS<sub>4.7</sub> as Mo<sup>4.7</sup>(S<sub>2</sub><sup>2-</sup>)<sub>2.35</sub>. Sulfur K-edge absorption spectra for MoS<sub>3</sub>, MoS<sub>4.7</sub>, sulfur, and the model compound VS<sub>4</sub> are in agreement with these formulations and assignment of oxidation states. Comparisons with crystalline materials are made and possible models of the structures presented.

## Introduction

The amorphous trichalcogenides, MoS<sub>3</sub>, WS<sub>3</sub>, MoSe<sub>3</sub>, and WSe<sub>3</sub>, have been known since 1825.<sup>1</sup> They have been considered as possible cathode materials in lithium cells,<sup>2</sup> and structural studies have been carried out by a number of workers. The comprehensive EXAFS study of Cramer *et al.*<sup>3</sup> suggested that the basic unit building block was the MX<sub>6</sub> unit and that the materials contained the metal in a lower oxidation state than 6. MoS<sub>3</sub>, for example, is often formulated as Mo<sup>V</sup>(S<sup>2-</sup>)<sub>2</sub>(S<sub>2</sub><sup>2-</sup>)<sub>0.5</sub>. Evidence for this comes from the short Mo–Mo distance consistent with a metal–metal bond, from vibrational spectroscopy which shows an S–S bond, and from photoelectron spectroscopy showing two different types of sulfur.<sup>4</sup> Several X-ray diffraction studies on MoS<sub>3</sub> and WS<sub>3</sub> have been carried out,<sup>5,6</sup> the study by Chien *et al.* being the most comprehensive.<sup>7</sup> In the latter study, a structure is proposed for MoS<sub>3</sub> which contains chains of face-sharing MoS<sub>6</sub> octahedra with alternate long and short Mo–Mo distances and the S–S units across the short, bonded distance as shown in Figure 1. This model includes long Mo–S<sup>-I</sup> bonds (2.60 Å) and short Mo–S<sup>-II</sup> bonds (2.40 Å). The chain model is also supported by the EXAFS

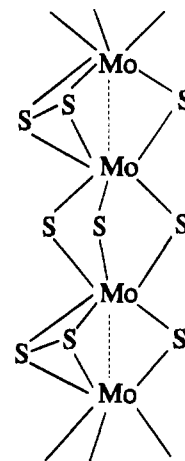


Figure 1. Single chain model proposed for MoS<sub>3</sub> by Chien *et al.*<sup>7</sup> The dotted line indicates a Mo–Mo bond.

studies of Huntley *et al.*<sup>8</sup> and Scott *et al.*,<sup>9</sup> who found a long nonbonded Mo–Mo distance of ~3.2 Å in addition to the short, bonded Mo–Mo distance of 2.75 Å. Müller *et al.* have proposed a model containing Mo<sub>3</sub> units<sup>10</sup> and have suggested that the reactions of MoS<sub>3</sub> provide evidence for this.<sup>11</sup> In addition to amorphous MoS<sub>3</sub>, hydrated MoS<sub>3</sub>·nH<sub>2</sub>O has been reported by a number of workers,<sup>12</sup> although the structure of this material does not appear to have been investigated.

<sup>®</sup> Abstract published in *Advance ACS Abstracts*, August 15, 1995.

- (1) Mellor, J. W. *A Comprehensive Treatise on Inorganic and Theoretical Chemistry*; Longman: London, 1931; Vol. 11, p 1437.
- (2) Jacobson, A. J.; Chianelli, R. R.; Rich, S. M.; Whittingham, M. S. *Mater. Res. Bull.* **1979**, *14*, 1437.
- (3) Cramer, S. P.; Liang, K. S.; Jacobson, A. J.; Chang, C. H.; Chianelli, R. R. *Inorg. Chem.* **1984**, *23*, 1215.
- (4) Liang, K. S.; de Neufville, J. P.; Jacobson, A. J.; Chianelli, R. R.; Betts, F. J. *Non-Cryst. Solids* **1980**, *35*, 1249.
- (5) Liang, K. S.; Cramer, S. P.; Jacobson, A. J.; Chang, C. H.; de Neufville, J. P.; Chianelli, R. R.; Betts, F. J. *Non-Cryst. Solids* **1980**, *42*, 345.
- (6) Diemann, E. Z. *Anorg. Allg. Chem.* **1977**, *432*, 127.
- (7) Chien, F. Z.; Moss, S. C.; Liang, K. S.; Chianelli, R. R. *Phys. Rev.* **1984**, *B29*, 4606.

- (8) Huntley, D. R.; Parham, T. G.; Merrill, R. P.; Sienko, M. J. *Inorg. Chem.* **1983**, *22*, 4144.
- (9) Scott, R. A.; Jacobson, A. J.; Chianelli, R. R.; Pan, W.-H.; Stiefel, E. I.; Hodgson, K. O.; Cramer, S. P. *Inorg. Chem.* **1986**, *25*, 1461.
- (10) Müller, A.; Fedin, V.; Hegetschweiler, K.; Amrein, W. J. *Chem. Soc., Chem. Commun.* **1992**, 1795.
- (11) Müller, A.; Diemann, E.; Krickemeyer, E.; Walberg, H.-J.; Bögge, H.; Armatage, A. *Eur. J. Solid State Inorg. Chem.* **1993**, *30*, 565.
- (12) Rode, E. Ya.; Lebedev, B. A. *Russ. J. Inorg. Chem.* **1961**, *6*, 608.

The tetrasulfide, MoS<sub>4</sub>, was first reported by Berzelius in 1825<sup>1</sup> and is mentioned in several inorganic textbooks, as well as in the *Dictionary of Inorganic Compounds*,<sup>13</sup> where it is formulated as MoS<sub>2</sub>(S<sub>2</sub>). Closer inspection of the literature reveals little concrete evidence on which to base this formulation.

We have recently prepared a number of new chalcogen-rich chalcogenides of chromium, molybdenum, and tungsten,<sup>14,15</sup> which include a compound with approximate composition MoS<sub>4</sub>. We are using neutron scattering<sup>16</sup> and EXAFS studies to elucidate the structures of these materials and, as part of our studies, have reinvestigated the structure of MoS<sub>3</sub>. In this paper, we report the structural results we obtained from the analysis of Mo K-edge EXAFS data for MoS<sub>4.7</sub>, MoS<sub>3</sub>, and MoS<sub>3</sub>·*n*H<sub>2</sub>O (*n* ~ 2) (prepared using a number of methods) and the evidence for the sulfur oxidation state and coordination from S K-edge absorption studies of MoS<sub>3</sub> and MoS<sub>4.7</sub> and the model compounds αS and VS<sub>4</sub>. VS<sub>4</sub> is a suitable model compound because all the sulfur is found in the -I oxidation state in one type of chemical environment as (μ<sub>2</sub>-η<sup>2</sup>-S<sub>2</sub>)<sup>2-</sup> groups.<sup>17</sup> This type of unit has been postulated to occur in MoS<sub>3</sub>; see Figure 1. On the basis of these investigations we propose structural models for MoS<sub>3</sub> and MoS<sub>4.7</sub>.

## Experimental Section

**(1) Sample Preparation and Characterization.** (a) **MoS<sub>3</sub> and MoS<sub>3</sub>·*n*H<sub>2</sub>O.** Using methods cited in the literature,<sup>12,18</sup> molybdenum trisulfide was prepared by four different routes:

(i) A ground sample of ammonium tetrathiomolybdate, (NH<sub>4</sub>)<sub>2</sub>MoS<sub>4</sub>, contained in a silica tube, was heated to 200 °C under dynamic vacuum for 24 h.

(ii) To an aqueous solution of ammonium tetrathiomolybdate, dilute hydrochloric acid was added until the solution became acidic (pH 1).

(iii) Sodium molybdate, Na<sub>2</sub>MoO<sub>4</sub>·2H<sub>2</sub>O (4.0 g), was dissolved in 100 mL of 2 M HCl, and H<sub>2</sub>S was passed through the resulting solution for 15 min.

(iv) Piperazine tetrathiomolybdate was synthesized by the addition of an aqueous solution of piperazine dihydrochloride monohydrate to an aqueous solution of ammonium tetrathiomolybdate. The resulting orange precipitate was isolated by filtration before being resuspended in water and decomposed with 2 M HCl.

The molybdenum trisulfide products obtained by methods ii–iv were obtained as aqueous suspensions. They were isolated by filtration and washed with 2 M HCl before being dried under vacuum. Fourier transform infrared spectra were recorded, on a Perkin Elmer 1720-X Fourier transform infrared interferometer, for each of the products. From these spectra we were able to confirm the purity of the compounds and the lack of starting materials in the final products. These spectra also show a broad peak centered at approximately 530 cm<sup>-1</sup> which is ascribed to the presence of (S–S)<sup>2-</sup> groups in the samples. Powder X-ray diffraction on an Inel Spectrolab Series 3000 diffractometer confirmed the compounds to be amorphous. Energy-dispersive X-ray analysis of individual particles, in a Philips CM20 transmission electron microscope equipped with an EDAX system, allowed their compositions to be determined. Compositions were determined, in the thin crystal limit, using the intensity ratios of the Mo L + S K peak to the Mo K peaks and a calibration curve determined using MoS<sub>2</sub> and (NH<sub>4</sub>)<sub>2</sub>MoS<sub>4</sub> standards. Methods i–iv gave products with the stoichiometry MoS<sub>3</sub> within experimental error (S/Mo = 3 ± 0.15). Magnetic susceptibilities

measured at room temperature on a Sherwood Scientific magnetic susceptibility balance showed MoS<sub>3</sub> to be diamagnetic.

The sample prepared by method i was found to be anhydrous, as expected, while the other three samples were all found to contain water. In order to ascertain the water content of each sample, small amounts (~0.2 g) of the compounds were oxidized to MoO<sub>3</sub> at 500 °C together with reference samples of molybdenum disulfide. The loss of mass upon oxidation enabled the water content of each sample to be determined. The results for the samples prepared by methods ii–iv gave the overall compositions, MoS<sub>3</sub>·1.7H<sub>2</sub>O, MoS<sub>3</sub>·2.1H<sub>2</sub>O, and MoS<sub>3</sub>·2.2H<sub>2</sub>O, respectively. The density of MoS<sub>3</sub> was determined using a liquid displacement density bottle and was found to be 3.1 g cm<sup>-3</sup>. The densities of MoS<sub>3</sub>·1.7H<sub>2</sub>O, MoS<sub>3</sub>·2.1H<sub>2</sub>O, and MoS<sub>3</sub>·2.2H<sub>2</sub>O were all found to be 2.6 g cm<sup>-3</sup>.

(b) **MoS<sub>4.7</sub>.** MoS<sub>4.7</sub> was prepared by the reaction of Mo(CO)<sub>6</sub> with sulfur in boiling 1,2-dichlorobenzene.<sup>14</sup> An excess of sulfur was employed (24:1 molar ratio); the unreacted sulfur was removed by washing with carbon disulfide. As with MoS<sub>3</sub>, the infrared spectrum of MoS<sub>4.7</sub> showed the presence of (S–S)<sup>2-</sup> groups, although the peak at 530 cm<sup>-1</sup> is more pronounced for MoS<sub>4.7</sub>. The composition of the amorphous material was again determined using energy-dispersive X-ray analysis in a transmission electron microscope to yield an average stoichiometry of MoS<sub>4.65(25)</sub>. This composition was in agreement with that determined using thermogravimetric analysis. Powder X-ray diffraction showed that washing in carbon disulfide had removed unreacted crystalline sulfur from the product, and differential scanning calorimetry confirmed that no amorphous or crystalline sulfur was present in the sample. The density was determined as 3.0 g cm<sup>-3</sup>. A room temperature magnetic susceptibility measurement on a Sherwood Scientific magnetic susceptibility balance showed MoS<sub>4.7</sub> to be diamagnetic.

**(2) Mo K-Edge EXAFS Spectroscopy.** Mo K-edge EXAFS data were collected in transmission mode on station 9.2 at the Daresbury Laboratory SRS, using a Si [220] crystal monochromator and 50% harmonic rejection. Ionization chambers, filled with a mixture of Ar/He or Kr/He, at appropriate partial pressures to optimize detector sensitivities, were placed in the beam path before and after the sample. Finely-ground samples were diluted in boron nitride to give a satisfactory edge jump and absorption. Data were collected at room temperature for all samples and also at low temperature for MoS<sub>3</sub> and MoS<sub>4.7</sub>.

S K-edge X-ray absorption spectra were measured by total electron yield on station 3.4 at the Daresbury Laboratory SRS, using a Si [111] monochromator. Samples were mixed with about 30% by volume of graphite to increase their electrical conductivity, dispersed in chloroform and painted onto stainless steel stubs to produce a continuous film. The samples were placed in a vacuum chamber, and spectra were collected under ultrahigh vacuum conditions.<sup>19,20</sup> The spectra were calibrated with respect to αS (2472 eV), which was repeatedly run to ensure that no shift in energy scale was occurring between measurements on the different samples.

## Data Analysis

The basic equation for the interpretation of EXAFS data is

$$\chi(k) = \sum_j \frac{N_j}{kR_j^2} |f_j(\pi)| e^{-2R_j/\lambda} e^{-2\sigma_j^2 k^2} \sin(2kR_j + 2\delta + \psi_j)$$

where  $\chi(k)$  is the magnitude of the X-ray absorption fine structure as a function of the photoelectron wave vector  $k$ .  $N_j$  is the coordination number and  $R_j$  the interatomic distance for the  $j$ th shell.  $\delta$  and  $\psi_j$  are phase shifts experienced by the photoelectron,  $f_j(\pi)$  is the amplitude of the photoelectron backscattering, and  $\lambda$  is the electron mean free path; these are

(13) Macintyre, J. E. *Dictionary of Inorganic Compounds*; Chapman and Hall Chemical Database; Chapman and Hall: 1992; Vol. 3, p 3594.

(14) Rice, D. A.; Hibble, S. J.; Almond, M. J.; Hassan Mohammad, K. A.; Pearse, S. P. *J. Mater. Chem.* **1992**, *2*, 895.

(15) Hibble, S. J.; Rice, D. A.; Almond, M. J.; Hassan Mohammad, K. A.; Pearse, S. P.; Sagar, J. R. *J. Mater. Chem.* **1992**, *2*, 1237.

(16) Hibble, S. J.; Pickup, D. M.; Hannon, A. C. *Phys. Scr.* **1995**, *T57*, 94.

(17) Allmann, R.; Baumann, I.; Kutoglu, A.; Röscher, H.; Hellner, E. *Naturwissenschaften* **1964**, *51*, 263.

(18) Debucquet, E.; Velluz, L. *Bull. Soc. Chim. Fr.* **1932**, *51*, 1571.

(19) MacDowell, A. A.; West, J. B.; Greaves, G. N.; Van der Laan, G. *Rev. Sci. Instrum.* **1988**, *59*, 843.

(20) Roper, M. D.; Buksh, P. A.; Kirkman, I. W.; Van der Laan, G.; Padmore, H. A.; Smith, A. D. *Rev. Sci. Instrum.* **1992**, *63*, 1322.

calculated within EXCURV92.<sup>21</sup> The Debye–Waller factor is represented by  $A = 2\sigma^2$  in EXCURV92.

We used the programs EXCALIB, EXBACK, and EXCURV92<sup>21</sup> to extract the EXAFS signal and analyze the data. Least squares refinements of the structural parameters of our compounds were carried out against the  $k^3$  weighted EXAFS signal to minimize the fit index, FI,

$$FI = \sum_i (k^3(\chi_i^T - \chi_i^E))^2$$

where  $\chi_i^T$  and  $\chi_i^E$  are the theoretical and experimental EXAFS, respectively. The results of refinements are reported in terms of the discrepancy index

$$R = \left( \int |\chi^T(k) - \chi^E(k)| k^3 dk / \int |\chi^E(k)| k^3 dk \right) \times 100\%$$

The Mo K-edge EXAFS data for all compounds were fitted to models consisting of Mo–S and Mo–Mo shells. The starting parameters used in the refinement were the distances from the EXAFS study of Cramer *et al.*<sup>3</sup> with six sulfurs in the first shell and one molybdenum in the second shell. An amplitude factor (AFAC) of 0.8, which allows for the reduction in the EXAFS amplitude due to multiple excitations, was employed in the data analysis. Refinement of  $R$ ,  $N$ , and  $A$  for both shells gave, for all samples of  $\text{MoS}_3$  and  $\text{MoS}_3 \cdot n\text{H}_2\text{O}$ , coordination numbers close to 6 and 1. In contrast, for the new sulfide,  $\text{MoS}_{4.7}$ , the comparable values were close to 7 and 1.3. It had previously been suggested in a study of  $\text{MoS}_3$ <sup>7</sup> that within the molybdenum coordination sphere there were two markedly different metal–sulfur distances. Refinements were carried out with a split sulfur shell in  $\text{MoS}_3$  in an attempt to improve the fit and ascertain if different Mo–S distances could be resolved. This gave no improvement in fit, and for further refinements we fixed the coordination numbers of the S and Mo shells for  $\text{MoS}_3$  at 6 and 1 and for  $\text{MoS}_{4.7}$  at 7.33 and 1.33, respectively. This allowed us to make meaningful comparisons of temperature factors for different compounds and for the same compound at different temperatures. These values could also be used to build chemically reasonable models for these materials.

S K-edge absorption spectra were produced from the raw data using the program EXCALIB and normalized to the absorption maxima to allow easy comparison of edge shifts and peak shapes.

## Results

**(1) Coordination around Molybdenum.** Figure 1a shows the  $k^3$  weighted EXAFS data for  $\text{MoS}_3$  and the theoretical curve produced from our model. Figure 2b shows the Fourier transform. Parts a and b of Figure 3 show the equivalent plots for  $\text{MoS}_3 \cdot 1.7\text{H}_2\text{O}$ , which are almost indistinguishable from those for  $\text{MoS}_3$ . The EXAFS data for the other hydrated samples are similarly indistinguishable from those for  $\text{MoS}_3$ . No evidence can be seen for backscattering from any other shells. Attempts to split the sulfur shell in  $\text{MoS}_3$  did not produce a statistically significant improvement in the fit index. Figure 4a shows the  $k^3$  weighted EXAFS data for  $\text{MoS}_{4.7}$  and the theoretical curve produced from our model, and Figure 4b, the Fourier transform. Table 1 shows the refined structural parameters obtained from Mo K-edge EXAFS on  $\text{MoS}_3$ ,  $\text{MoS}_3 \cdot n\text{H}_2\text{O}$  ( $n = 1.7, 2.1, \text{ and } 2.2$ ), and  $\text{MoS}_{4.7}$ .

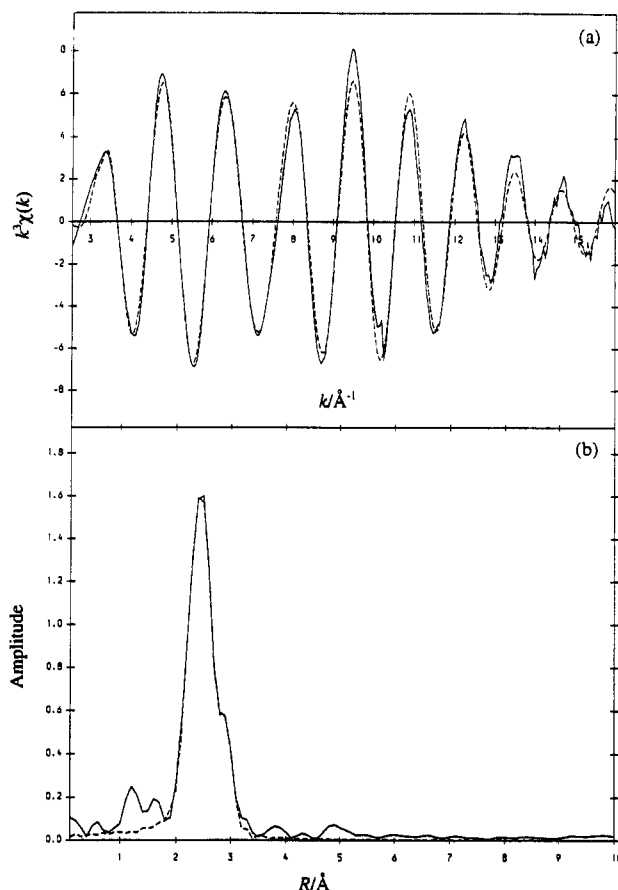


**Figure 2.** Mo K-edge EXAFS data for  $\text{MoS}_3$  at 80 K: (a)  $k^3$  weighted EXAFS experimental (—) and theoretical (---) curves,  $R = 17.03\%$ , and (b) the Fourier transform phase corrected using the first shell (Mo–S) backscattering factor.

**(2) Oxidation State of Sulfur.** The normalized S K-edge EXAFS spectra for  $\text{MoS}_3$ ,  $\text{MoS}_{4.7}$ ,  $\text{VS}_4$ , and  $\alpha\text{S}$  are shown superimposed on each other in Figure 5. Significant changes in both the position of the absorption edges and in the peak shapes for the different compounds can be seen. The simplest interpretation is that the absorption edge shifts to higher energy as the oxidation state of sulfur increases. This should be an even better approximation when sulfur is found in similar environments.

## Discussion

The EXAFS results for  $\text{MoS}_3$  and all the  $\text{MoS}_3 \cdot n\text{H}_2\text{O}$  samples are very similar, but the differences in coordination numbers for  $\text{MoS}_3$  and  $\text{MoS}_{4.7}$  are significant. Fixing the coordination numbers close to the values to which they were initially refined allows us to compare the temperature factors for the two types of material.

For all the compounds, the temperature factors ( $A = 2\sigma^2$ ) for the molybdenum shell are similar and are close to the values expected from the model for a diatomic harmonic oscillator<sup>22</sup> with a vibrational wave number of  $200\text{ cm}^{-1}$  (a reasonable estimate for the value expected for a Mo–Mo stretch),<sup>23</sup> which gives  $A = 0.008\text{ Å}^2$ . They show the temperature dependence expected for weak bonds, with  $A$  falling by  $0.004\text{ Å}^2$  between 300 and 80 K. The values obtained for the  $A$  factors for both compounds are of the order expected for purely thermal disorder.

(21) Binsted, N.; Campbell, J. W.; Gurman, S. J.; Stephenson, P. C. *EXAFS analysis program*; Daresbury Laboratory: Warrington, U.K., 1991.

(22) Teo, B. K. *EXAFS: Basic Principles and Data Analysis*; Springer-Verlag: Berlin, 1986; p 99.

(23) Nakamoto, K. *Infra-red and Raman Spectra of Inorganic and Coordination Compounds*, 4th ed.; Wiley: New York, 1986; p 336.

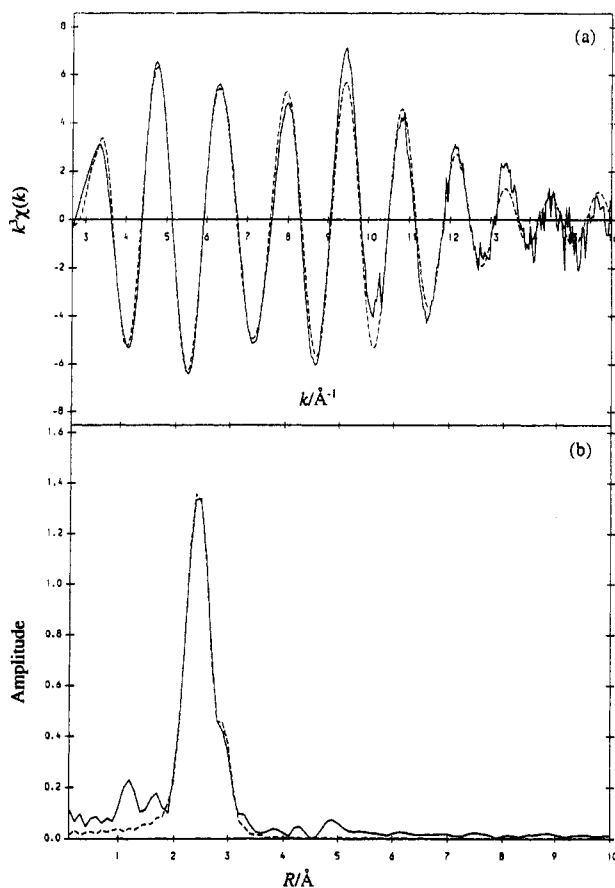


**Figure 3.** Mo K-edge EXAFS data for  $\text{MoS}_3 \cdot 1.7\text{H}_2\text{O}$  at 300 K: (a)  $k^3$  weighted EXAFS experimental (—) and theoretical (---) curves,  $R = 19.47\%$ , and (b) the Fourier transform phase corrected using the first shell (Mo–S) backscattering factor.

The  $A$  factors for the sulfur shells are larger than for the molybdenum shells. In this case it seems likely that there are two contributions, the effect of thermal disorder and the effect of static disorder arising from variation in Mo–S bond lengths, i.e.,

$$A_{\text{total}} = A_{\text{thermal}} + A_{\text{static}}$$

The contribution from thermal disorder can be estimated by the change in  $A$  occurring on cooling from 300 to 80 K. The change in  $A$  for  $\text{MoS}_{4.7}$  could be modeled by a simple diatomic harmonic oscillator with a vibrational wave number,  $\nu_{\text{Mo-S}}$ , of  $350 \text{ cm}^{-1}$ , which is typical for a Mo–S bond.<sup>24</sup> The  $A$  parameters calculated using this model would be 0.006 and  $0.004 \text{ \AA}^2$  at 300 and 80 K, respectively. The static disorder resulting from variation in the Mo–S distances is clearly much larger in  $\text{MoS}_3$  than in  $\text{MoS}_{4.7}$ .

The information on distances, coordination numbers, and Debye–Waller factors can be used to construct simple models for these compounds and bring into doubt some of the earlier models presented in the literature for  $\text{MoS}_3$ .

(1)  $\text{MoS}_3$ . The refined parameters are consistent with two irregular octahedral  $\text{MoS}_6$  units sharing a face, with a short,  $2.76 \text{ \AA}$ , Mo–Mo distance across this face. However, there is no evidence that these units are linked into longer chains by further face sharing nor evidence for the formation of  $\text{Mo}_3$  triangles. Earlier EXAFS studies<sup>3,8,9</sup> were carried out over a greater  $k$  range. This results in better resolution of the Mo–S

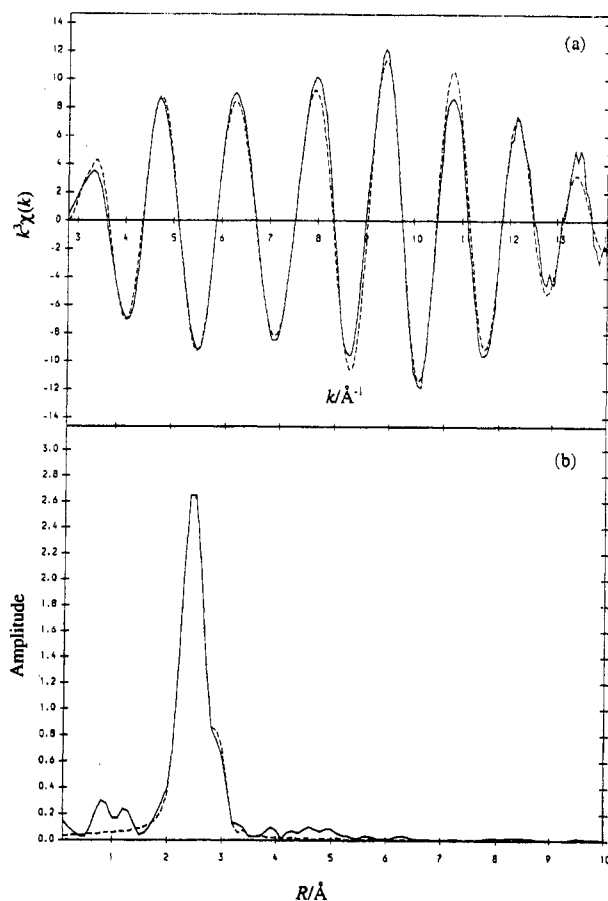


**Figure 4.** Mo K-edge EXAFS data for  $\text{MoS}_{4.7}$  at 80 K: (a)  $k^3$  weighted EXAFS experimental (—) and theoretical (---) curves,  $R = 13.15\%$ , and (b) the Fourier transform phase corrected using the first shell (Mo–S) backscattering factor.

**Table 1.** Coordination Numbers ( $N$ ), Distances ( $R$ ), and Debye–Waller ( $A$ ) Factors Obtained from the EXAFS Study of  $\text{MoS}_3$ ,  $\text{MoS}_3 \cdot n\text{H}_2\text{O}$ , and  $\text{MoS}_{4.7}$ <sup>a</sup>

compound	temp/K	shell	$N^b$	$R^c/\text{\AA}$	$A/\text{\AA}^2$	$R/\%$
(i) $\text{MoS}_3$ (fit range $2.8\text{--}16 \text{ \AA}^{-1}$ )	300	Mo–S	6	2.43	0.015	15.73
		Mo–Mo	1	2.75	0.008	
	80	Mo–S	6	2.43	0.012	17.03
		Mo–Mo	1	2.75	0.004	
(ii) $\text{MoS}_3 \cdot 1.7\text{H}_2\text{O}$ (fit range $2.8\text{--}16 \text{ \AA}^{-1}$ )	300	Mo–S	6	2.43	0.014	19.47
		Mo–Mo	1	2.77	0.006	
(iii) $\text{MoS}_3 \cdot 2.1\text{H}_2\text{O}$ (fit range $2.8\text{--}14 \text{ \AA}^{-1}$ )	300	Mo–S	6	2.43	0.015	19.85
		Mo–Mo	1	2.77	0.010	
(iv) $\text{MoS}_3 \cdot 2.2\text{H}_2\text{O}$ (fit range $2.8\text{--}13 \text{ \AA}^{-1}$ )	300	Mo–S	6	2.43	0.016	18.36
		Mo–Mo	1	2.78	0.007	
$\text{MoS}_{4.7}$ (fit range $2.8\text{--}14 \text{ \AA}^{-1}$ )	300	Mo–S	7.33	2.44	0.010	16.12
		Mo–Mo	1.33	2.77	0.006	
	127	Mo–S	7.33	2.44	0.008	11.56
		Mo–Mo	1.33	2.77	0.004	
	80	Mo–S	7.33	2.44	0.008	13.15
		Mo–Mo	1.33	2.78	0.003	

<sup>a</sup> Note that  $R$  is the discrepancy index and i–iv refer to the preparative methods described in the Experimental Section. <sup>b</sup> The absolute accuracy of coordination numbers derived from EXAFS is 10–20%. See text for discussion of relative values for these materials, which were fixed after preliminary data analysis. <sup>c</sup> Distances are estimated to be accurate to  $\pm 0.01\text{--}0.02 \text{ \AA}$ , allowing for errors in data collection and analysis.

and bonded Mo–Mo distance but cannot be used to explain the absence of the longer ( $\sim 3.2 \text{ \AA}$ ) Mo–Mo distance in our study. It is possible that the longer distance seen in earlier EXAFS studies was a result of  $\text{MoS}_2$  impurities produced in the thermal decomposition route used to prepare it. It should be noted that  $\text{MoS}_3 \cdot n\text{H}_2\text{O}$ , which is discussed below, is prepared

(24) Müller, A.; Nolte, W. O.; Krebs, B. *Angew. Chem., Int. Ed. Engl.* **1978**, *17*, 279.

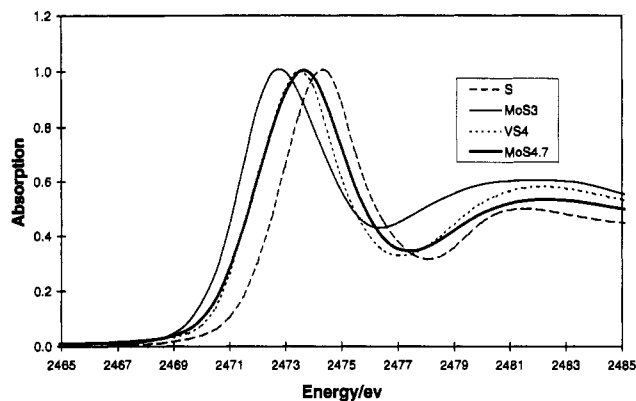


Figure 5. Normalized S K-edge absorption spectra for MoS<sub>3</sub>, MoS<sub>4.7</sub>, VS<sub>4</sub>, and  $\alpha$ S.

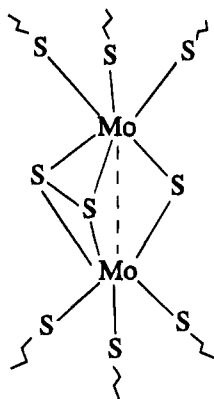


Figure 6. Mo<sub>2</sub>S<sub>9</sub> unit proposed as the basic building block in MoS<sub>3</sub>. The dotted line indicates a Mo–Mo bond. Jagged lines show bonds to molybdenum atoms in other units.

at lower temperatures and decomposition to form MoS<sub>2</sub> is even less likely. The interpretation of the X-ray data as evidence for the formation of long chains by sharing two faces of the octahedra, the model proposed by Chien,<sup>7</sup> is not satisfactory, as S–S nonbonded distances are not considered. Approximately six of these distances at 3.4 Å would account for the peak in the radial pair distribution function ascribed to a Mo–Mo distance of 3.39 Å. This postulated Mo–Mo distance is the only evidence other than that from EXAFS for the two-face-sharing model. Furthermore, we would expect to see a longer Mo–Mo distance if a second face were shared, as this mode of interconnection would lead to a fairly rigid unit with a low Mo *A* factor. Our EXAFS experiments suggest that the linking together of the basic Mo<sub>2</sub>S<sub>9</sub> units (Figure 6) must occur by vertex or edge sharing of the octahedra. This would lead to longer Mo–Mo distances and a large *A* factor, because of the flexibility of these types of links. Both of these would reduce the backscattering amplitude from the nonbonded second Mo shell and explain why we see no evidence for this distance in our results. We are carrying out neutron and X-ray diffraction experiments in an attempt to obtain independent confirmation of the model we propose for the mode of linkage between Mo<sub>2</sub>S<sub>9</sub> units. The large *A* parameter for the sulfur shell is probably due to the variation in bond lengths caused by the presence of both S<sup>-I</sup> and S<sup>-II</sup> in the basic structural unit. The position, to lower energy than VS<sub>4</sub>, and width, with a tail to lower energy, of the S K-edge absorption edge for MoS<sub>3</sub> supports the conclusion that the majority of the sulfur is S<sup>-II</sup> with some S<sup>-I</sup>. This is in agreement with the formulation of MoS<sub>3</sub> as Mo<sup>V</sup>(S<sup>2-</sup>)<sub>2</sub>(S<sub>2</sub><sup>2-</sup>)<sub>0.5</sub>. The diamagnetism of the compound is explained by the pairing of electrons from Mo<sup>V</sup> (d<sup>1</sup>) to form the Mo–Mo bond in the Mo<sub>2</sub>S<sub>9</sub> unit.

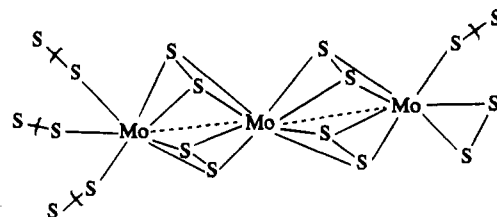


Figure 7. Mo<sub>3</sub>S<sub>14</sub> unit proposed as the basic building block in MoS<sub>4.7</sub>. The dotted line indicates a Mo–Mo bond. Sulfurs outside the brackets belong to other units.

(2) MoS<sub>3</sub>·*n*H<sub>2</sub>O. The close similarity of the EXAFS signal and derived parameters for MoS<sub>3</sub> and the MoS<sub>3</sub>·*n*H<sub>2</sub>O samples suggests that the basic molybdenum–sulfur framework is identical in the two materials. It seems likely that the water is physically occluded in the MoS<sub>3</sub>·*n*H<sub>2</sub>O samples. There is, for example, no evidence for any Mo–O bonds which would occur if water was directly coordinated to molybdenum. Comparison of the densities of MoS<sub>3</sub> and MoS<sub>3</sub>·*n*H<sub>2</sub>O is revealing. The density of the MoS<sub>3</sub>·*n*H<sub>2</sub>O samples is slightly higher than that calculated assuming MoS<sub>3</sub> occupies the same volume as in anhydrous MoS<sub>3</sub>, and H<sub>2</sub>O, the same volume as in liquid water. For example the density of MoS<sub>3</sub>·2H<sub>2</sub>O would be calculated to be 2.3 g cm<sup>-3</sup>. This discrepancy (measured value 2.6 g cm<sup>-3</sup>) can be explained if we assume that the water molecules are also able to occupy some of the vacant space in the amorphous MoS<sub>3</sub> framework.

(3) MoS<sub>4.7</sub>. The sulfur coordination number of 7.33 suggests a mixture of 7 and 8 coordination for molybdenum in MoS<sub>4.7</sub>. The overall stoichiometry can be satisfied by linking a central 8 coordinate molybdenum atom to two 7 coordinate molybdenum atoms in a linear chain, as shown in Figure 7. This gives the correct average coordination numbers and the correct overall stoichiometry if the central Mo shares two S<sub>2</sub><sup>2-</sup> units with each terminal Mo. The central molybdenum atom would be nominally Mo<sup>IV</sup>, and the terminal molybdenum atoms would be Mo<sup>V</sup>. This would mean all the sulfur was present as S<sup>-I</sup>, and it implies the formula Mo<sup>4.7</sup>(S<sub>2</sub><sup>2-</sup>)<sub>2.35</sub>. The lower *A* factor for the sulfur shell in MoS<sub>4.7</sub> relative to MoS<sub>3</sub> can be understood as reflecting the fact that all the sulfur is in the same oxidation state, leading to less variation in the Mo–S bond lengths. This structure resembles that of the [Mo<sub>2</sub>(S<sub>2</sub>)<sub>6</sub>]<sup>2-</sup> ion.<sup>24,25</sup> Interestingly, the amount of static disorder present in this ion, calculated from the X-ray data, is identical to the static disorder contribution to the *A* factor for the sulfur shell in MoS<sub>4.7</sub> after subtraction of the estimated thermal contribution. The diamagnetism of MoS<sub>4.7</sub> can be explained by the pairing of the 4 electrons in the Mo<sub>3</sub> unit (2 × Mo<sup>V</sup> (d<sup>1</sup>) + Mo<sup>IV</sup> (d<sup>2</sup>)) to form the two Mo–Mo bonds shown in Figure 6.

The shift in position of the S K-edge absorption edge, shown in Figure 5, is consistent with the average oxidation state of sulfur being higher in MoS<sub>4.7</sub> than in MoS<sub>3</sub>. The S K-edge absorption spectrum for MoS<sub>4.7</sub> clearly confirms that it is not a mixture of MoS<sub>3</sub> and sulfur.

**Acknowledgment.** We thank the University of Reading Endowment Fund for a studentship for D.M.P., the EPSRC for funding M.P.B., EXAFS facilities, and the grant for the electron microscope, and I. D. Fawcett, G. van Dorssen, and A. D. Smith for help with the EXAFS and X-ray absorption experiments.

IC950065G